# Supplementary Information

# Direct observation of the intermediate in an ultrafast isomerization.

Tyler M. Porter[1†], Jiaxi Wang[1†], Yingmin Li[1], Bo Xiang[1], Catherine Salsman[1], Joel S. Miller[2], Wei Xiong[1]*, and Clifford P. Kubiak[1]*.

[1]Department of Chemistry and Biochemistry, University of California San Diego, 9500 Gilman Drive, La Jolla, California 92093-0358, United States.

[2]Department of Chemistry, University of Utah, 315 South 1400 East, Room 2124, Salt Lake City, Utah 84112-0850.

**Materials and Methods:**

**Preparation and Purification**: The 2,3-hexafluorobutyne was used as received from Oakwood Chemicals while the triruthenium doedecacarbonyl and triphenyl phosphine was used as received from Acros Organics. The cyclohexane stabilized dichloromethane (DCM), was purchased from VWR International LLC, deoxygenated and dried over alumina columns on a custom built solvent system under an argon atmosphere and stored over activated 4 Å molecular seives in a nitrogen filled glove box. The 2,3-dithiolene and $Ru(S_2C_2(CF_3)_2)(CO)(PPh_3)_2$ were prepared following modified literature reported proceudures.[1] In brief:

**Bis(perfluoromethyl)-1,2-dithietene.** In accord with literature,[2] in a well ventilated fumehood, a 2 neck round bottom flask equipped with a short path distillation head was charged with 25 g (97.46 mmol) of sulfer and heated to 325 ºC under a nitrogen stream. Upon reaching 325 ºC, the 2,3-hexafluorobutyne was bubbled through the molten sulfer in short puffs and the dithietene was collected in a receiving Schlenk flask as a red-tinted oil.

**$Ru(S_2C_2(CF_3)_2)(CO)(PPh_3)_2$.** Under an inert atmosphere a 250 mL Schlenk flask was charged with 400 mg (0.63 mmol) of triruthenium dodecacarbonyl, 580 mg (2.57 mmol) of bis(perfluoromethyl)-1,2-dithietene, and approximately 100 mL of *n*-heptane that was heated under reflux. After 45 minutes, following carbon monoxide evolution an orange solid had precipitated. The flask was cooled and the orange solid was collected by vacuum filtration, washed with *n*-heptane, and dried under vacuum. The orange solid, tentatively identified as $Ru_2(S_2C_2(CF_3)_2)(CO)_6$ [359 mg (0.60 mmol)], was then added to a flask containing 1.1427 g (4.36 mmol) of triphenylphosphine suspended in 50 mL of *n*-heptane. After heating to reflux for 12 hours, the flask was cooled to 0 ºC and the crystalline complex was collected by filtration. Futher purification was achieved by recrystalization for dichloromethane/hexanes solutions where a mixture of orange and violet crystals were obtained.

**Infrared Data Collection and Analysis**. Infrared spectra were collected on a Bruker Equinox 55 FTIR spectrometer using a SPECAC flow through optical cryostat (model, 21525) with a 1.12 mm path length (determined from infringing pattern), $CaF_2$ windowed cell enclosed in a vacuum jacketed housing. Solutions were prepared in a glove box under a nitrogen atmosphere using pre-dried DCM from a mixture of orange and violet crystals. Cell temperature (± 1 °C) was regulated by addition of liquid nitrogen/methanol to the cooling compartment and heating to the desired temperature with a computer controlled thermocouple/heating coil system. Both solutions of the complex and solvent blanks were recorded at temperature ranging from 20 °C to –80 °C to ensure accurate solvent subtraction. To obtain the integrated spectral areas for the exchanging species, spectral curve fitting was carried out in MATLAB (version 9.1.0.44655). The ν(CO) bands were fit by constraining three Gaussian functions ± 4 $cm^{-1}$ centered around 1940, 1960, and 1980 $cm^{-1}$ for all temperatures, while fixing a fourth Gaussian centered at 1920 $cm^{-1}$.

**UV/visible Data Collection and Analysis**. Cryostatic UV-visible spectra were collected on a Shimadzu UV–3600 UV/vis/NIR spectrometer, using the same cell setup described above for FTIR data collection. Samples were contained in SPECAC sealed liquid FTIR cells with $CaF_2$ crystal optic windows and a path length of 1.12 mm. Spectral curve fitting was carried out in MATLAB (version 9.1.0.44655).

**Density Functional Theory Analysis.** Calculations were performed in the ORCA software suite (version 3.0.3) at the BP86 level of theory with the RIJCOSX approximation.[3-7] Ruthenium, phosphorous, sulfur, and oxygen atoms were treated with the DEF2-TZVP/J basis sets while DEF2-SVP/J was used for all other atoms.[8-16] Dispersion corrections were applied using the atom-pairwise dispersion correction with a Becke-Johnson damping scheme (D3BJ) and solvation was accounted for using the COSMO solvation model in methylene chloride.[17-19] Analytical frequency calculations were performed at the same level of theory and molecular graphics were performed with the UCSF Chimera package.[20]

**NMR Data Collection and Analysis**. $^{1}H$ NMR spectra were recorded on a JEOL 500 MHz NMR spectrometer and analyzed using iNMR software. A total of 64 scans of 32768 data points were collected from from –185 to 185 ppm. $^{31}P$ spectra were recorded in predried dichloromethane-$d_2$ solutions from 25 to – 80 °C.

**2DIR Experimental Set up, Data Collection, and Analysis**. 2D IR spectra were collected in pump-probe geometry.[21-22] The pulse sequence is described in Figure S2. In brief, three mid-IR pulses were sent to interact with the sample, where two vibrational coherences were created during $t_1$ and $t_3$ period. To generate the pulse sequence, 800nm laser pulses (~35 fs, ~6 W, 1 kHz) were generated by ultrafast Ti:Sapphire regenerative amplifier (Astrella, Coherent) . The 800nm was converted into mid-IR pulses by optical parametric amplifier (TOPAS, Coherent) followed by a different frequency generation process on a Type II $AgGaS_2$ crystal (Eksma). The mid-IR pulse (30 μJ) was split into two beams by a beam-splitter. The majority (95%) was sent into a Ge-AOM based pulse shaper (QuickShape Kit, PhaseTech) to prepare the two pump pulse in the pulse sequences, whereas 5% mid-IR served as the probe.[21-22] The pump pulse pair (2 μJ at the sample), the probe (<0.5 μJ) were all focused and spatially overlapped on the sample by a f = 10 cm parabolic mirror and collimated by another parabolic mirror in a symmetric geometry.

In the 2D IR experiments, two vibrational coherences were generated during $t_1$ and $t_3$ periods, respectively. The first coherence was measured by scanning $t_1$ time from 0 to 2000 fs in

steps of 20 fs using the pulse shaper, where a rotating frame at $f_0$=1583 $cm^{-1}$ was used to shift the oscillation period to 80 fs, so that the scanning step can meet with the Nyquist frequency requirement. In order to detect the 2D IR signal (the second vibrational coherence) by the CCD camera (256×1,024, Andor), the collimated signal and the probe beam were then upconverted by a residue 800 nm beam on a 5%Mg: $LiNbO_3$ crystal.[23-24] Since the 800 nm served as a window function, the $t_3$ time delay were covered by the upconversion process and the 800 nm pulse duration determined how long $t_3$ was "scanned".[25-26] The up-converted 2D IR signals were experimentally Fourier transformed by a spectrograph and detected by a CCD camera. To get full absorptive 2D IR spectra, the first vibrational coherence was numerical Fourier transformed along $t_1$ axis. The pump and probe pulses had the same polarization in 2D IR measurements. For the time dependent 2D IR measurements, $t_2$ was scanned by a computerized delay stage.

**Obtaining Chemical Exchange Rate Constants from Time Dependent 2D IR Spectra.** The volume of each peak with respect to $t_2$ was obtained from the $t_2$-dependent 2D IR spectra.[27-28] As shown in Figure S3, multiple Gaussian functions were used to fit the 2D IR spectral cut along the probe axis at the peak 2 frequency (~1940 $cm^{-1}$) on the pump axis. All 2D IR spectra at different $t_2$ times were fit following the same method. Each Gaussian function represents one species in the 2D IR spectrum. For example, at $t_2$ = 0 ps, the single Gaussian was used to fit the positive peak of the spectral cut corresponding to the fundamental transition of diagonal peak 2. Similarly, at $t_2$ = 25 ps, three Gaussians were needed to account for the cross peaks resulting from chemical exchange. Peak volumes for each species were obtained from the Gaussian fitting parameters, assuming a circular 2D Gaussian distribution for each peak component. In the generalized transition of a species A to B, the lower corner cross peak of the diagonal peak ratios in the 2D IR spectrum can be expressed as functions of $t_2$. [29]

$$\frac{S_{BA}}{S_{AA}} = \frac{1 - e^{-(k_{AB} + k_{BA})\cdot t_2}}{1 + \frac{k_{AB}}{k_{BA}}\cdot e^{-(k_{AB} + k_{BA})\cdot t_2}}$$

$$= \frac{1 - e^{-k_{sum}\cdot t_2}}{1 + K_{eq(A\leftrightarrow B)}\cdot e^{-k_{sum}\cdot t_2}}$$

The sum of the rate constants of a transition ($k_{for}$ + $k_{rev}$) was directly obtained from fitting $S_{cross\ peak}$ /$S_{diagonal\ peak}$ with respect to $t_2$. Given the $K_{eq}$ from VT-FTIR data in Table 1, $k_{for}$ and $k_{rev}$ can be calculated separately (Figure S4).

**Summary of a Three-Site Exchange Process**:

Consider three isomers exchanging in a triangular fashion:

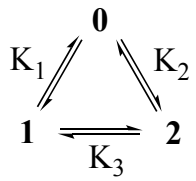

$$K_1 = \frac{k_1}{k_{-1}} \qquad K_2 = \frac{k_2}{k_{-2}} \qquad K_3 = \frac{k_3}{k_{-3}}$$

The kinetic equations for a three-site exchange are:

$$\frac{d[1]}{dt} = k_{-1}[0] - k_1[1] + k_{-3}[2] - k_3[1] \tag{1}$$

$$\frac{d[0]}{dt} = k_1[1] - k_{-1}[0] - k_2[0] + k_{-2}[2] \tag{2}$$

$$\frac{d[2]}{dt} = k_2[0] - k_{-2}[2] + k_3[1] - k_{-3}[2] \tag{3}$$

The mass balance for the system is:

$$[1]_0 = [1] - [0] - [2] \tag{4}$$

Applying a Laplace Transform to the kinetic equations we obtain:

$$P[1] - P[1]_0 = k_{-1}[0] - k_1[1] + k_{-3}[2] - k_3[1] \tag{5}$$

$$P[0] = k_1[1] - k_{-1}[0] - k_2[0] + k_{-2}[2] \tag{6}$$

$$P[2] = k_2[0] - k_{-2}[2] + k_3[1] - k_{-3}[2] \tag{7}$$

Which can be written as:

$$\begin{pmatrix} P + k_1 + k_3 & -k_{-1} & -k_{-3} \\ -k_1 & P + k_{-1} + k_2 & -k_{-2} \\ -k_3 & -k_2 & P + k_{-2} + -k_{-3} \end{pmatrix} \cdot \begin{pmatrix} [1] \\ [0] \\ [2] \end{pmatrix} = \begin{pmatrix} [1]_0 \\ 0 \\ 0 \end{pmatrix} \tag{8}$$

$$\begin{pmatrix} [1] \\ [0] \\ [2] \end{pmatrix} = \begin{pmatrix} P + k_1 + k_3 & -k_{-1} & -k_{-3} \\ -k_1 & P + k_{-1} + k_2 & -k_{-2} \\ -k_3 & -k_2 & P + k_{-2} + -k_{-3} \end{pmatrix}^{-1} \cdot \begin{pmatrix} [1]_0 \\ 0 \\ 0 \end{pmatrix} \tag{9}$$

Using MATLAB and the inverse Laplacian transform, the above expressions could be solved analytically when the experimental values for the exchange constants are used. This allowed for the determination of the concentration profiles for **1**, **0**, and **2** as a function of time (Figure S12). When the analysis above is used for [**1**], [**0**], and [**2**] with the extracted time constants (Table S1) we can plot the concentrations of **1**, **0**, and **2**, as a function of time assuming $[\mathbf{1}]_0$ = 0.01 M and $[\mathbf{0}]_0 = [\mathbf{1}]_0$ = 0 M (Figure S12). When starting with species **1** only, and fitting the concentration profile of **2** to a simple exponential model (eq. 10), the concentration profile of **2** presents a time constant of 3 ps which occurs on a much faster time scale than the observed 2D IR cross peak dynamics for the direct conversion of **1** to **2** (8.6 (2.0) ps).

$$[2] = b - ae^{\frac{-t}{\tau}} \tag{10}$$

While this data does not directly support that the origin of the 2D IR cross peak for the isomerization of **1** to **2** is due to direct chemical exchange, further evidence is shown by

increasing the time constant, $\tau_{12}$ from 8.6 ps to 750 ps effectively removing this pathway from the isomerization process (Fig S14). When $\tau_{12}$ = 750 ps, the concentration profile of **2** presents a time constant of 13.0 (4) ps: a value within experimental error of the 2D IR observed exchange time constant. Furthermore, when the pathway $K_{12}$ is removed entirely and the expressions are solved for a traditional three-site exchange problem (Figure S12) fits of **2** present a time constant of 13.4 (4) ps. This is in excellent agreement with the results from triangle exchange and within experimental error of the 2D IR observed time constant (Fig S12). These data suggest that while a definitive answer remains undetermined, given literature precedent, DFT calculations (*vide infra*), and the kinetic analysis presented here, it is unlikely that the dynamics of the direct **1** to **2** exchange process can compete with those involving the faster interconversions that pass through **0** as an intermediate.

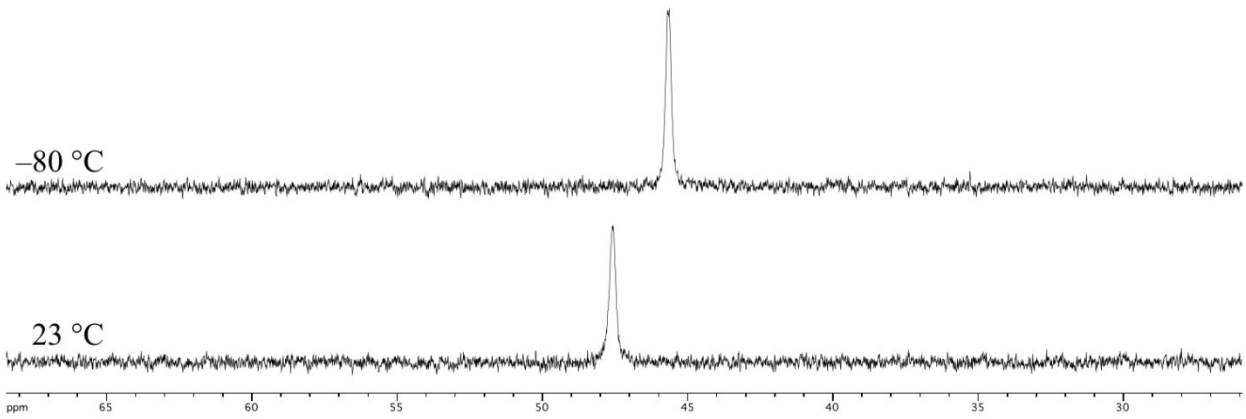


**Figure S1.** Variable temperature $^{31}P$ NMR in DCM-$d_2$.

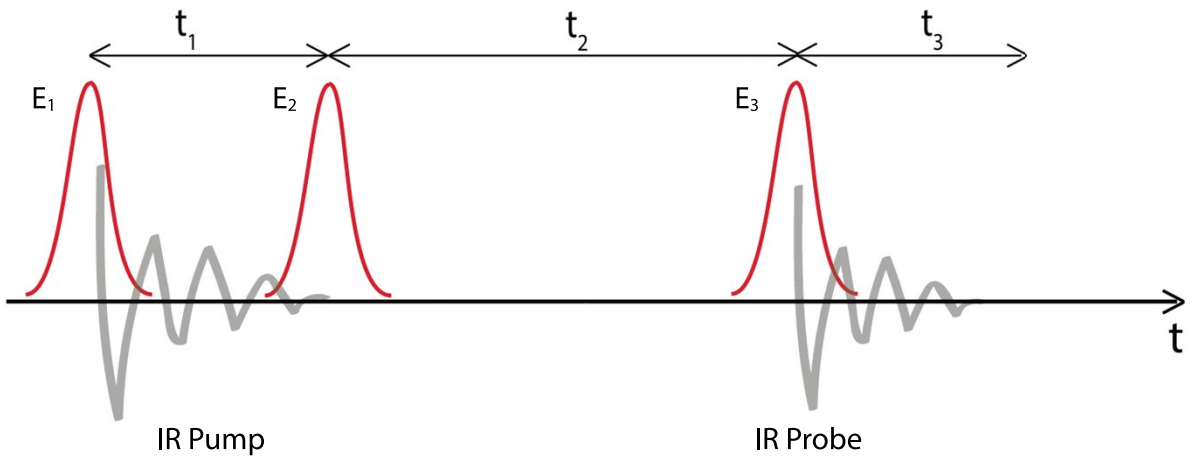


**Figure S2.** Pulse sequence used in 2D IR experiment.

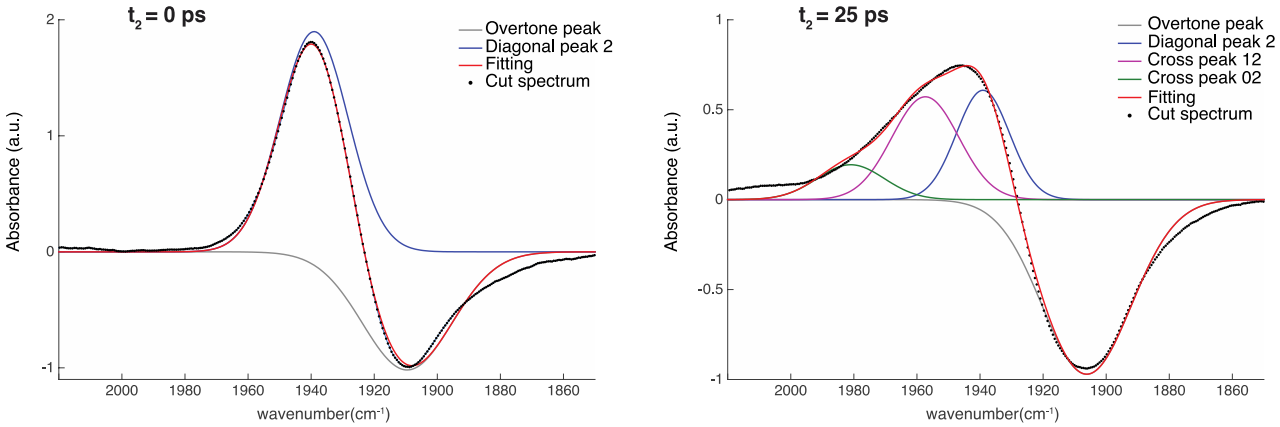


**Figure S3** (Left) Cut $t_2 = 0$ ps 2D IR spectrum along probe axis at peak 2 on pump axis. Two Gaussian functions: a negative overtone peak and diagonal peak 2 were used to fit the spectrum; (Right) Cut $t_2 = 25$ ps 2D IR spectrum along probe axis at peak 2 on pump axis. Four Gaussian functions: a negative overtone peak, diagonal peak 2, cross peak 12, and cross peak 02 were used to fit the cut spectrum.

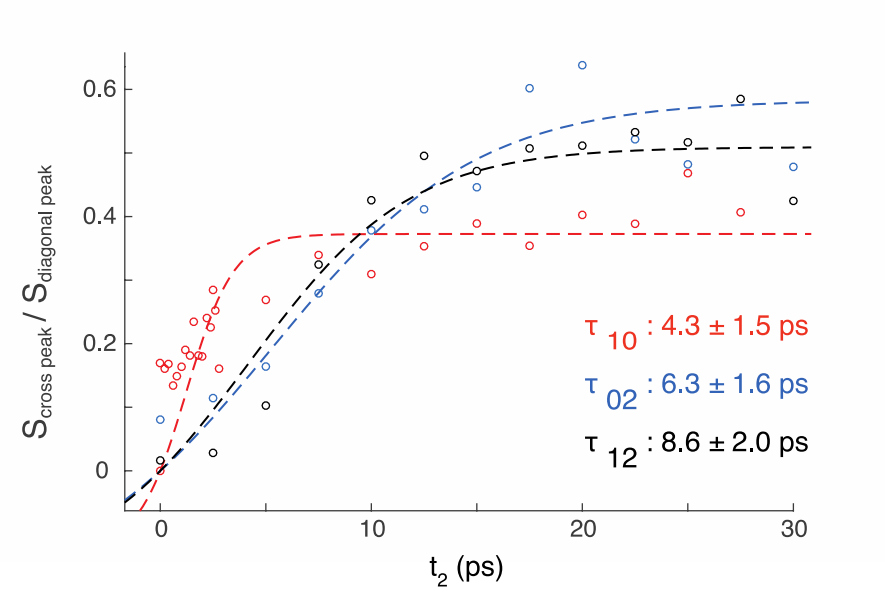


**Figure S4.** Cross peak ratios at varies $t_2$ time delays. Dots are experimental results; dashed lines are experimental results fitted to chemical exchange model. Time constant of each dynamic exchange process is extracted from the increasing cross peak ratio over $t_2$.

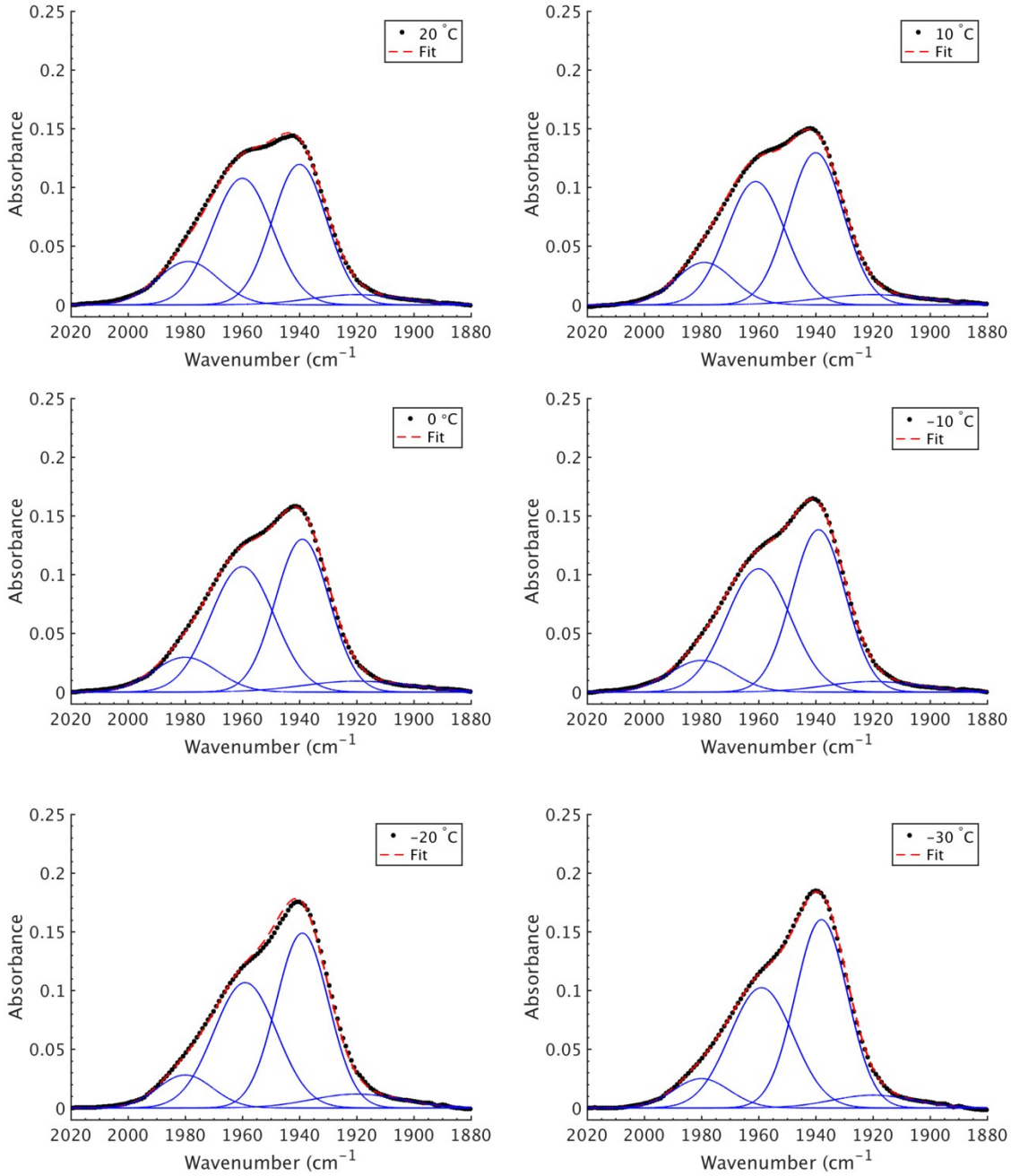


**Figure S5.** VTFTIR fits of ν(CO) bands for 0 (1980 $cm^{-1}$), 1 (1960 $cm^{-1}$), and 2 (1940 $cm^{-1}$) isomers ranging from 20 to –30 °C in DCM. Black traces are experimental data while the red traces are the sum of the Gaussian functions use to fit the ν(CO) bands.

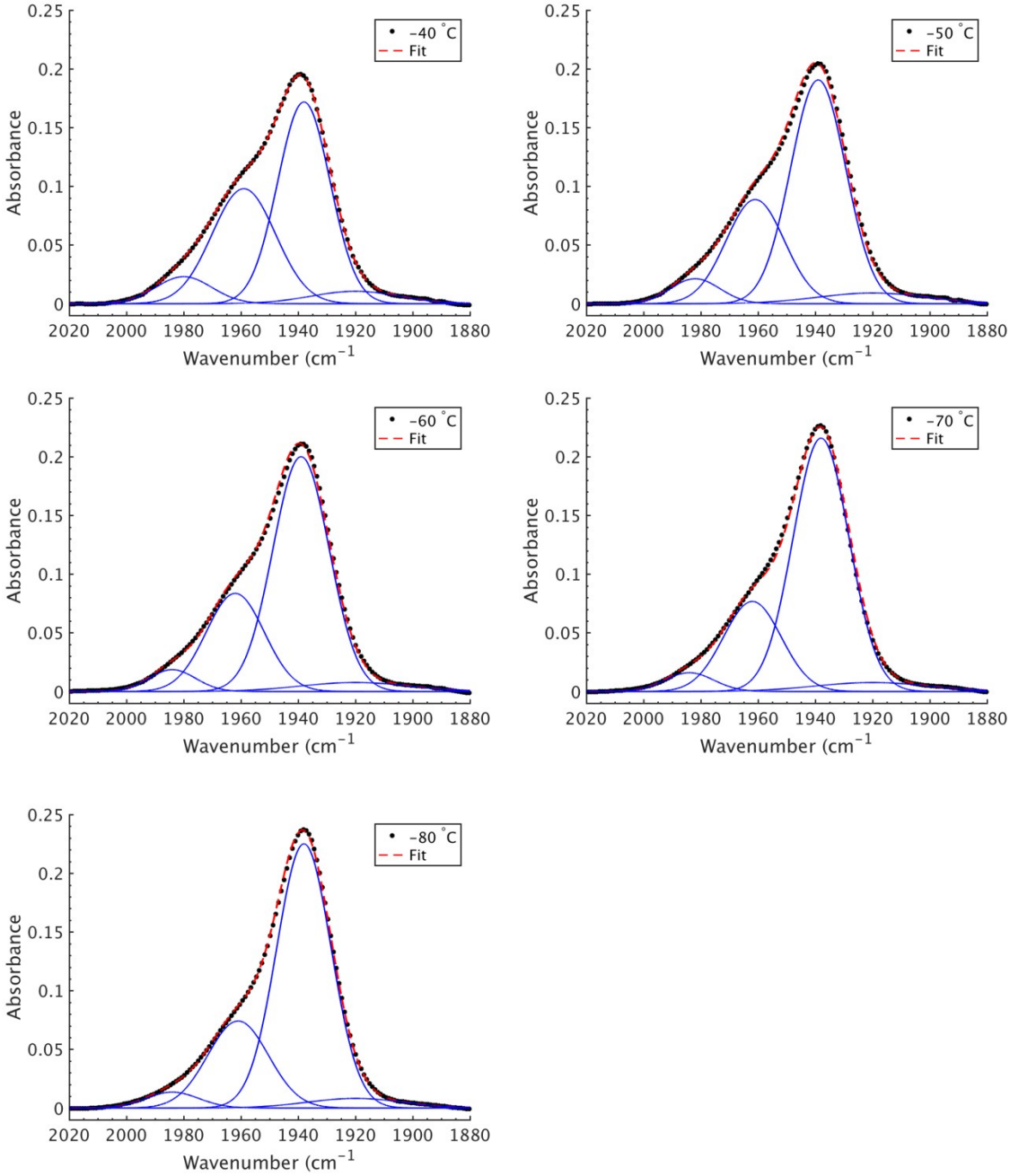


**Figure S6.** VTFTIR fits of ν(CO) bands for **0** (1980 $cm^{-1}$), **1** (1960 $cm^{-1}$), and **2** (1940 $cm^{-1}$) isomers ranging from –40 to –80 °C in DCM. Black traces are experimental data while the red traces are the sum of the Gaussian functions use to fit the ν(CO) bands.

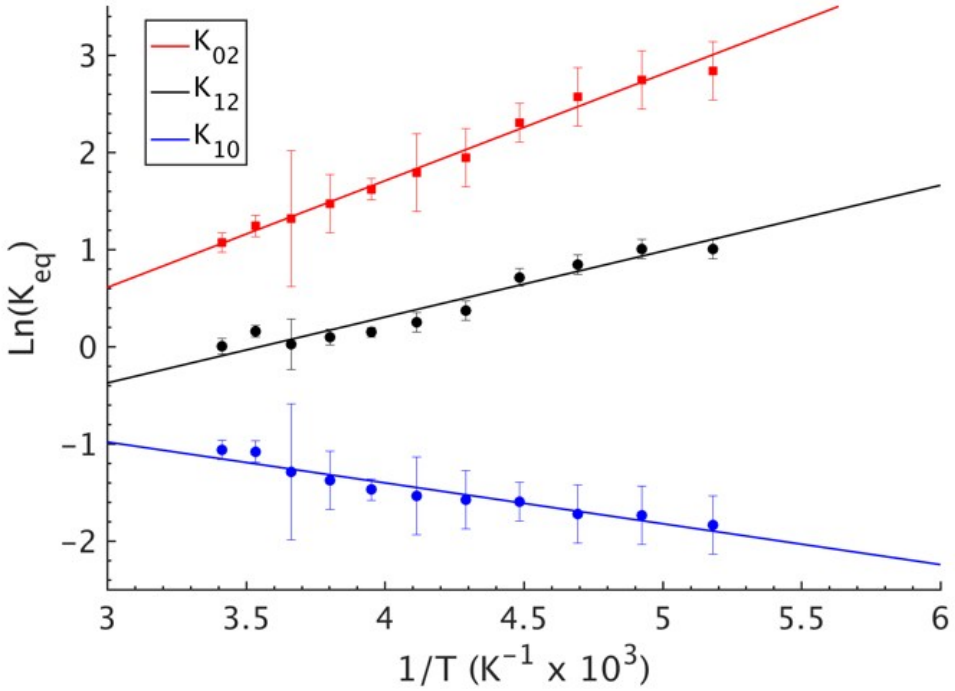


**Figure S7.** Plot of $Ln(K_{eq})$ vs. 1/T for the isomerization reaction. $K_{10}$ represents the equilibrium constant for exchange between **1** and **0**, $K_{02}$ represents the equilibrium constant for exchange between **0** and **2**, and $K_{12}$ represents the equilibrium constant for exchange between **1** and **2**.

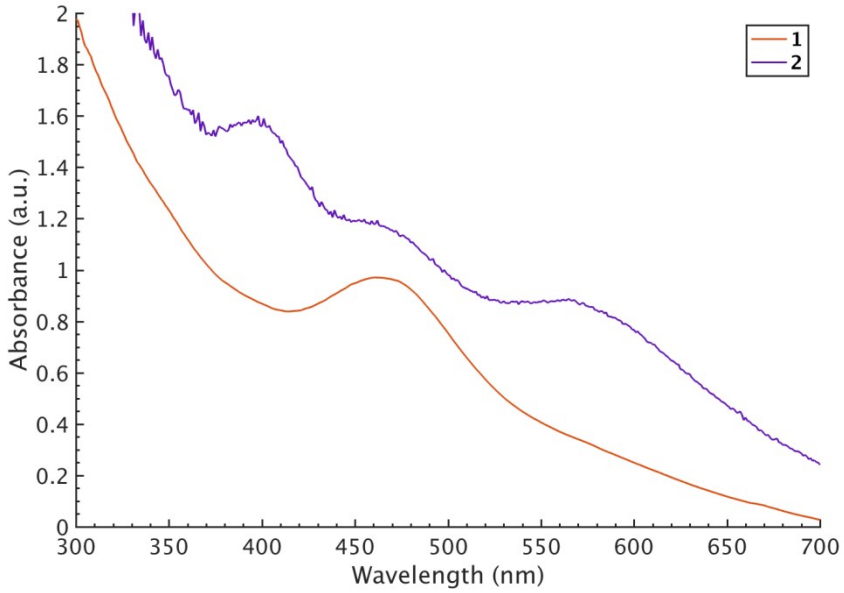


**Figure S8.** Solid state UV/vis spectroscopy taken in a KBr pellet. The orange isomer has a single absorbance maximum at 466 nm, while the violet isomer has three absorbance maxima at 396, 460, and 571 nm.

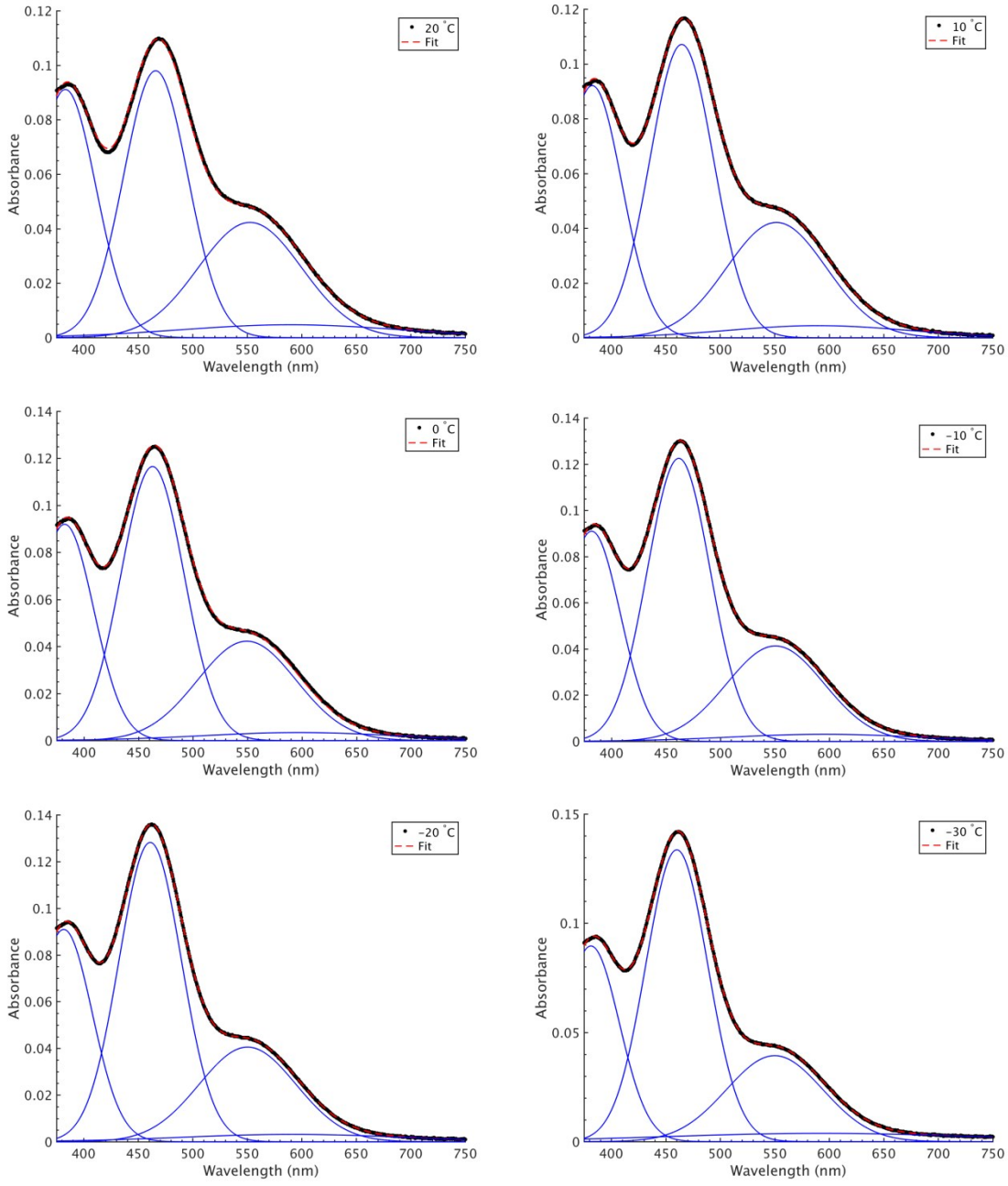


**Fig S9.** VTFT–UV/vis fits of **1** (385 and 561 nm), and **2** (470 nm) ranging from 20 to –30 °C in DCM. Black traces are experimental data while the red traces are the sum of the Gaussian functions use to fit the absorbance bands.

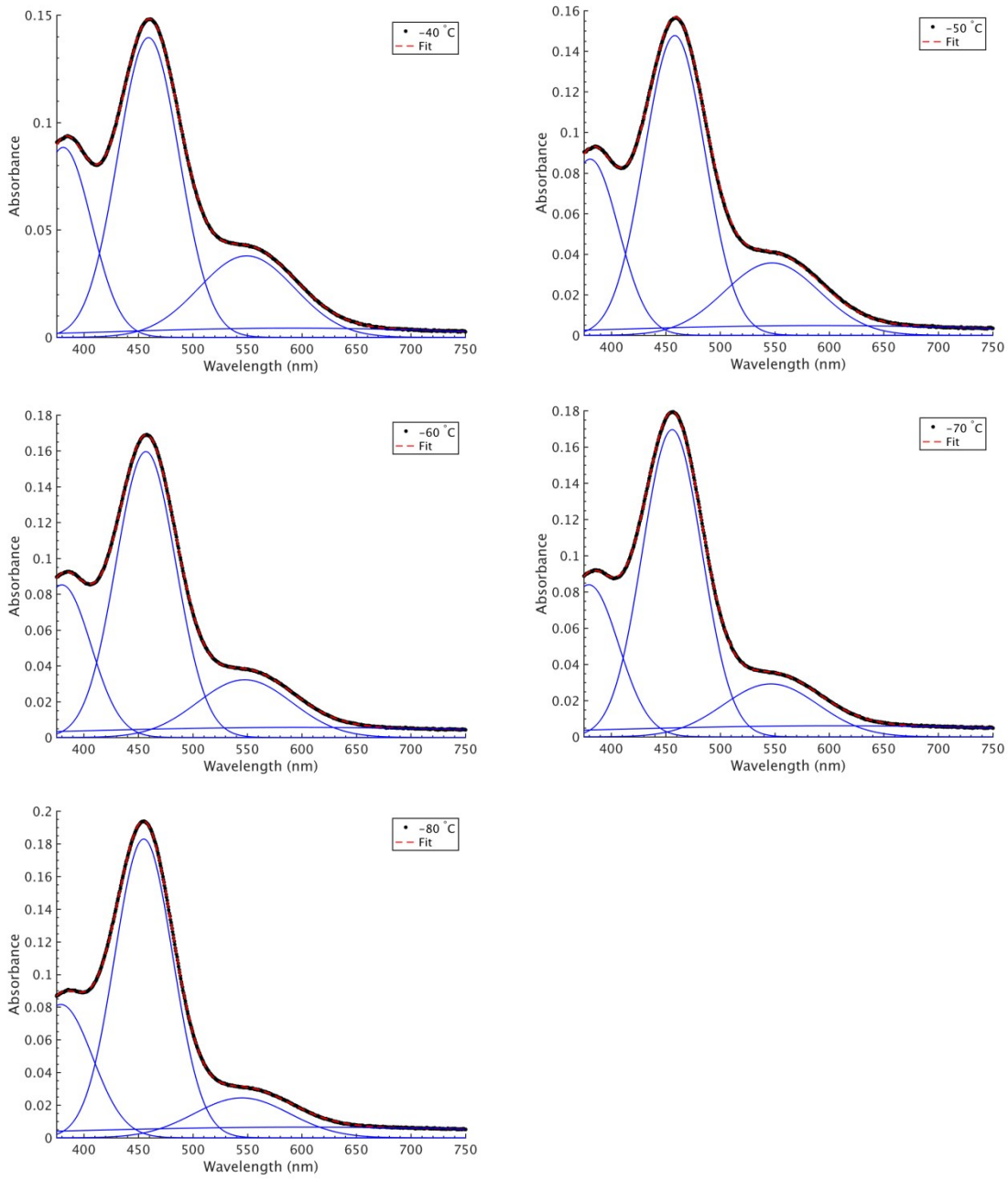


**Figure S10.** VTFT–UV/vis fits of **1** (385 and 561 nm), and **2** (470 nm) ranging from –40 to –80 °C in DCM. Black traces are experimental data while the red traces are the sum of the Gaussian functions use to fit the absorbance bands.

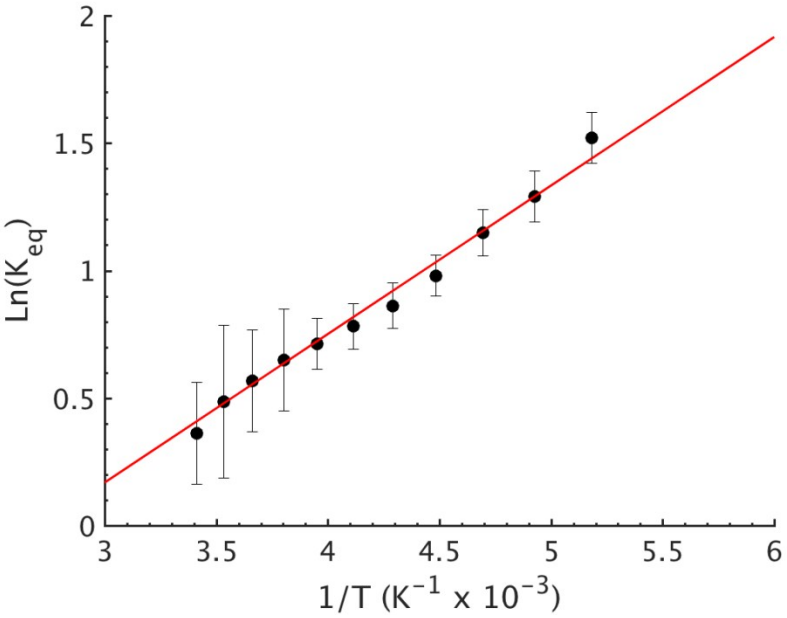


**Figure S11.** Plot of $Ln(K_{12})$ vs 1/T as obtained from UV/vis spectral analysis. $\Delta H$ and $\Delta S$ were found to be –1.21 kcal $mol^{-1}$ (0.04) and –3.4 (0.2) eu respectively.

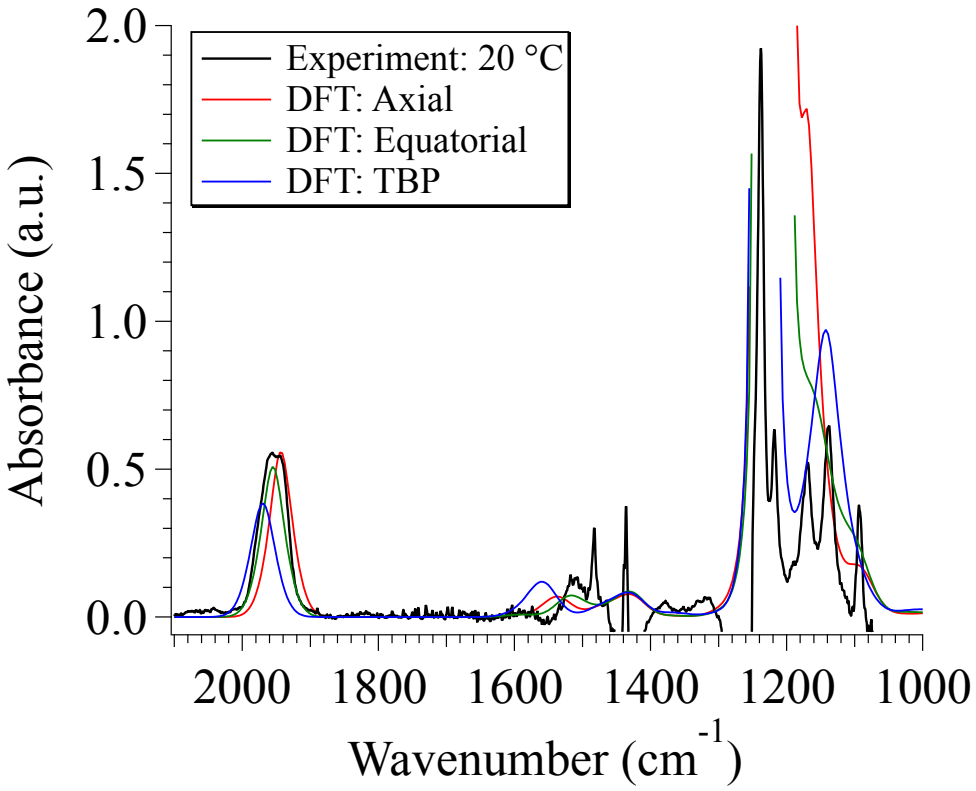


**Figure S12.** Comparison of experimental FTIR spectrum of $Ru(S_2C_2(CF_3)_2)_2(CO)(PPh_3)_2$ in DCM (Black) at 20 °C versus the DFT predicted FTIR spectra for the axial (Red), equatorial (Green), and TBP (Blue) isomers.

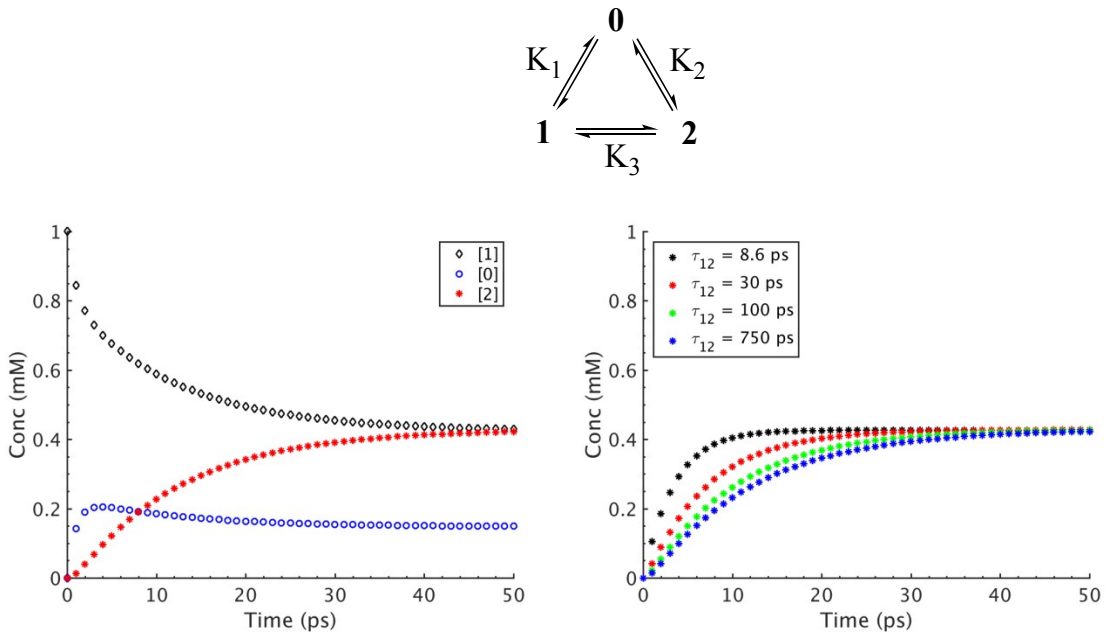


**Figure S13.** (left) Concentration profiles of **0** (black, diamonds), **1** (blue, circles), and **2** (red, stars), as a function of time as determined by analytically solving a triangular equilibrium. (right). Concentration profiles of **0** (circles), **1** (diamonds), and **2** (stars), as a function of time as with increasing $\tau_{12}$ (Black: $\tau_{12}$ = 8.6 ps; Red: $\tau_{12}$ = 30 ps; Green: $\tau_{12}$ = 100 ps; Blue: $\tau_{12}$ = 750 ps;).

$$\mathbf{1} \underset{k_{-1}}{\overset{k_1}{\rightleftharpoons}} \mathbf{0} \underset{k_{-2}}{\overset{k_2}{\rightleftharpoons}} \mathbf{2}$$

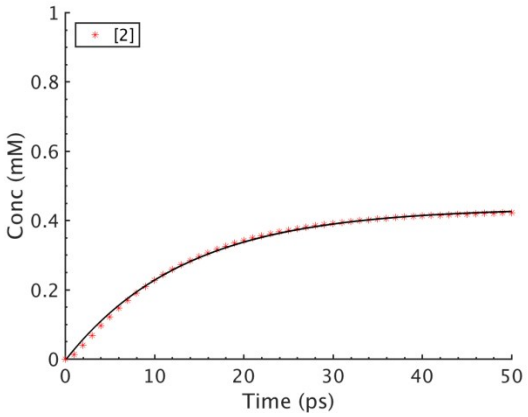


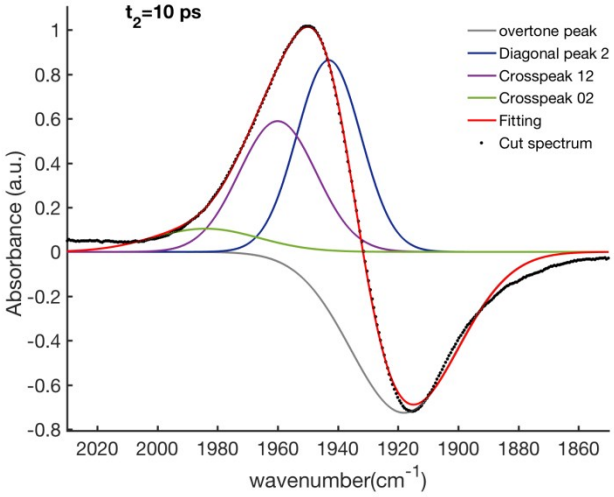


**Figure S14.** (top left) Concentration profiles of **0** (black, diamonds), **1** (blue, circles), and **2** (red, stars), as a function of time as determined by analytically solving a triangular equilibrium. (top right). Concentration profile of **2** (stars) as a function of time as with an exponential model supporting a time constant of 13.4 (4) ps. (bottom) 1D time resolved IR spectra at $t_2$ = 10 ps.

**Table S1.** Summary of time constants extracted from 2D IR and VT-FTIR experiments.

| | $K_{eq}$ | $\tau_f$ (ps) | $\tau_r$ (ps) |
|---|---|---|---|
| $K_{01}$ | 0.35 (0.03) | 4.3 (1.5) | 1.5 (0.5) |
| $K_{02}$ | 2.9 (0.2) | 6.3 (1.6) | 18.3 (4.9) |
| $K_{12}$ | 1.0 (0.1) | 8.6 (2.0) | 8.6 (2.0) |

**Table S2**. DFT optimized coordinates for **1.**

| Atom | X | Y | Z |
|---|---|---|---|
| Ru | 7.79680545 | 0.28691966 | 4.03017032 |
| S | 6.35419174 | -0.4945637 | 2.4019877 |
| S | 9.38800141 | -1.0652198 | 3.0502921 |
| P | 9.24729366 | 0.38064417 | 5.84038194 |
| P | 7.92997405 | 2.31308775 | 3.04270057 |
| O | 5.44057485 | 0.95264338 | 5.83540582 |
| C | 6.37687289 | 0.75834727 | 5.1235762 |
| C | 8.62659668 | -1.7651348 | 1.65049005 |
| C | 7.31836582 | -1.4551154 | 1.33250977 |
| C | 9.56096847 | -2.5795092 | 0.78296909 |
| C | 6.6256474 | -1.9294274 | 0.0672735 |
| F | 8.93584038 | -3.5981021 | 0.1585599 |
| F | 10.5624937 | -3.1147766 | 1.50825169 |
| F | 10.1477722 | -1.8167983 | -0.179554 |
| F | 5.49370808 | -1.2391488 | -0.1683427 |
| F | 6.28342123 | -3.2353798 | 0.13793524 |
| F | 7.41800787 | -1.773032 | -1.0173741 |
| C | 6.45488275 | 3.36237022 | 3.3110813 |
| C | 5.19313358 | 2.74670676 | 3.15060478 |
| C | 4.01939121 | 3.49481104 | 3.30577328 |
| C | 4.0912426 | 4.86057455 | 3.63951257 |
| C | 5.34379342 | 5.47872844 | 3.79120363 |
| C | 6.52478053 | 4.73510341 | 3.61734787 |
| C | 7.98379651 | 2.12975494 | 1.21497605 |
| C | 8.88651352 | 1.22061319 | 0.62663343 |
| C | 8.90471059 | 1.03590649 | -0.7633264 |
| C | 8.01691081 | 1.75399471 | -1.5816637 |
| C | 7.12627898 | 2.67495629 | -1.0036086 |
| C | 7.10933739 | 2.86448574 | 0.38785025 |
| C | 9.37510809 | 3.36878031 | 3.41448485 |
| C | 10.4084757 | 3.55656161 | 2.47026431 |
| C | 11.5569409 | 4.28830036 | 2.81343452 |
| C | 11.6773294 | 4.85656457 | 4.09356071 |
| C | 10.636949 | 4.70137461 | 5.02663161 |
| C | 9.49641994 | 3.9564176 | 4.69202276 |
| C | 11.0033917 | 0.08600124 | 5.43122035 |

| | | | |
|---|---|---|---|
| C | 11.7879079 | -0.8658301 | 6.11009691 |
| C | 13.1332824 | -1.0546923 | 5.75072176 |
| C | 13.7011525 | -0.2919378 | 4.71479694 |
| C | 12.9200561 | 0.66238379 | 4.03795057 |
| C | 11.5754332 | 0.84333318 | 4.38852087 |
| C | 8.79380889 | -1.0328803 | 6.92615492 |
| C | 8.57265985 | -0.887563 | 8.30961374 |
| C | 8.18934823 | -1.996907 | 9.08413863 |
| C | 8.03486691 | -3.2585021 | 8.48454486 |
| C | 8.26777408 | -3.4104929 | 7.10477398 |
| C | 8.63533195 | -2.3032687 | 6.32678084 |
| C | 9.2942367 | 1.79865397 | 6.99524775 |
| C | 8.08868455 | 2.41233637 | 7.40038405 |
| C | 8.11163416 | 3.5092665 | 8.27453441 |
| C | 9.33838297 | 4.00712601 | 8.75185969 |
| C | 10.5395329 | 3.3922284 | 8.36093342 |
| C | 10.5180137 | 2.29366328 | 7.48575686 |
| H | 5.14548082 | 1.68634361 | 2.87294878 |
| H | 3.04598044 | 3.00772635 | 3.17125059 |
| H | 3.17100532 | 5.44142531 | 3.77651934 |
| H | 5.40747071 | 6.54418165 | 4.04296923 |
| H | 7.49639301 | 5.23180058 | 3.71546957 |
| H | 9.5577933 | 0.63809173 | 1.26682049 |
| H | 9.58809917 | 0.29825273 | -1.1943402 |
| H | 8.0152078 | 1.59184316 | -2.6669988 |
| H | 6.4338982 | 3.24611844 | -1.6344531 |
| H | 6.4058238 | 3.58150514 | 0.82558876 |
| H | 10.3249128 | 3.12214386 | 1.46879912 |
| H | 12.3568064 | 4.41704039 | 2.07401425 |
| H | 12.5761729 | 5.42502439 | 4.36157169 |
| H | 10.7128752 | 5.14984055 | 6.02307223 |
| H | 8.69955241 | 3.82603997 | 5.42961816 |
| H | 11.3500048 | -1.4613888 | 6.92016374 |
| H | 13.7372755 | -1.8012424 | 6.2811065 |
| H | 14.7502965 | -0.444019 | 4.43289165 |
| H | 13.3542352 | 1.26014331 | 3.22709329 |
| H | 10.9624155 | 1.57653041 | 3.85733292 |
| H | 8.69990933 | 0.09065089 | 8.78781825 |
| H | 8.0119195 | -1.8714793 | 10.1594467 |

| | | | |
|---|---|---|---|
| H | 7.73369953 | -4.1222793 | 9.08973316 |
| H | 8.15441053 | -4.3929058 | 6.62967994 |
| H | 8.81450149 | -2.4103097 | 5.24917262 |
| H | 7.12924385 | 2.04323722 | 7.02799989 |
| H | 7.16886303 | 3.97999093 | 8.57723626 |
| H | 9.35593795 | 4.8717426 | 9.42674533 |
| H | 11.4998101 | 3.77317163 | 8.72852809 |
| H | 11.4597047 | 1.82989102 | 7.17331971 |

**Table S3**. DFT optimized coordinates for **2.**

| Atom | X | Y | Z |
|---|---|---|---|
| C | 0.75721833 | 0.08376497 | 3.95099892 |
| C | 2.09840308 | -0.9671104 | 8.28409063 |
| C | 2.01862371 | -0.5169075 | 9.61374308 |
| C | 1.57532464 | 0.78958612 | 9.88460999 |
| C | 1.2145817 | 1.64421792 | 8.83023828 |
| C | -0.1836932 | 3.61566425 | 6.87628907 |
| C | 0.33684542 | 4.88469655 | 7.20101304 |
| C | -0.4949124 | 5.86771867 | 7.76240915 |
| C | -1.8461382 | 5.58705071 | 8.02570083 |
| C | -2.3623829 | 4.31173228 | 7.7352937 |
| C | -1.54102 | 3.33624761 | 7.15443508 |
| C | 2.40329136 | 3.05052042 | 5.60589741 |
| C | -0.6686573 | 4.43387647 | 3.31841518 |
| C | -1.8265487 | 4.55386413 | 4.11755567 |
| C | -2.2480548 | 5.81206406 | 4.56968668 |
| C | -1.5064656 | 6.96177526 | 4.24756799 |
| C | -0.3547714 | 6.85029632 | 3.4497362 |
| C | 0.05958275 | 5.59242362 | 2.98103813 |
| C | -1.2405548 | 2.35732245 | 1.39154244 |
| C | -1.0827503 | 1.08763812 | 0.79560437 |
| C | -1.8654675 | 0.72611888 | -0.3082128 |
| C | -2.8224701 | 1.62491937 | -0.8174235 |
| C | 3.62614778 | 2.38737814 | 5.84125827 |
| C | -2.9867996 | 2.88585673 | -0.221106 |
| C | -2.1947604 | 3.2539731 | 0.88120338 |
| C | 1.46591901 | 2.87677573 | 2.01576069 |
| C | 2.59941018 | 2.22217693 | 2.52978322 |
| C | 3.84067789 | 2.33544749 | 1.88500221 |
| C | 3.96107192 | 3.10840771 | 0.71853592 |
| C | 2.82861875 | 3.75047279 | 0.18427403 |
| C | 1.58543804 | 3.62619436 | 0.82306753 |
| C | -3.5358505 | 0.02517995 | 4.80492312 |
| C | -2.9401183 | -0.4588281 | 5.94758453 |
| C | 4.82947568 | 2.93172101 | 5.3639521 |
| C | -3.6625764 | -1.2741036 | 7.00393042 |
| C | -4.943119 | -0.319098 | 4.36390976 |

| | | | |
|---|---|---|---|
| C | 4.8296464 | 4.15248164 | 4.66690107 |
| C | 3.61713967 | 4.82713768 | 4.44584277 |
| C | 2.41410805 | 4.2762064 | 4.90728662 |
| C | 1.29212943 | 1.19653682 | 7.4974495 |
| C | 1.72769899 | -0.1187461 | 7.23000192 |
| F | -5.3780201 | 0.51639964 | 3.39959815 |
| F | -5.8265071 | -0.2373779 | 5.3853603 |
| F | -5.0197937 | -1.5733115 | 3.86298364 |
| F | -4.4717119 | -0.4940799 | 7.7563345 |
| F | -4.4246973 | -2.2469151 | 6.45891018 |
| F | -2.7990292 | -1.8733192 | 7.84723796 |
| H | 2.43942167 | -1.9857149 | 8.06464155 |
| H | 2.29817352 | -1.1847542 | 10.4375481 |
| H | 1.50642101 | 1.14585286 | 10.9200044 |
| H | 0.86741561 | 2.66113452 | 9.046895 |
| H | 1.3929326 | 5.11264906 | 7.02342468 |
| H | -0.0804785 | 6.85528836 | 7.99778511 |
| H | -2.4944925 | 6.35944756 | 8.45691412 |
| H | -3.4125798 | 4.07814359 | 7.94680076 |
| H | -1.9362908 | 2.34076477 | 6.92301235 |
| H | -2.3917382 | 3.65067541 | 4.37735807 |
| H | -3.1473166 | 5.88948639 | 5.19078834 |
| H | -1.8243946 | 7.94304573 | 4.61970575 |
| H | 0.22777255 | 7.74288664 | 3.19201529 |
| H | 0.963876 | 5.51580199 | 2.36602598 |
| H | -0.3495092 | 0.38253542 | 1.20803873 |
| H | -1.7362086 | -0.2612313 | -0.7679049 |
| H | -3.4394634 | 1.33994397 | -1.6785804 |
| H | 3.64225041 | 1.4369375 | 6.38625695 |
| H | -3.7327521 | 3.58883164 | -0.6123163 |
| H | -2.3265738 | 4.23849663 | 1.34474431 |
| H | 2.51951465 | 1.62496677 | 3.43923695 |
| H | 4.71429111 | 1.82278592 | 2.30319775 |
| H | 4.93260127 | 3.20151201 | 0.21771849 |
| H | 2.90940196 | 4.33780495 | -0.7381333 |
| H | 0.69988446 | 4.1041394 | 0.38657389 |
| H | 5.77124368 | 2.39952551 | 5.54384593 |
| H | 5.77117162 | 4.57363653 | 4.29521687 |
| H | 3.6029923 | 5.77789943 | 3.90066592 |

| | | | |
|---|---|---|---|
| H | 1.47401476 | 4.79645408 | 4.70879667 |
| H | 1.77402787 | -0.4803864 | 6.19705349 |
| O | 1.5031744 | -0.7524942 | 3.52956649 |
| P | -0.1696821 | 2.73745073 | 2.83045367 |
| P | 0.81959092 | 2.28470131 | 6.10246138 |
| Ru | -0.5103068 | 1.21695799 | 4.55259235 |
| S | -2.6198811 | 1.00609527 | 3.69232351 |
| S | -1.298859 | -0.0418948 | 6.33472173 |

**Table S4**. DFT optimized coordinates for **0.**

| Atom | X | Y | Z |
|---|---|---|---|
| Ru | 8.24542705 | 0.0187036 | 3.76830521 |
| S | 6.94444952 | -0.8250444 | 1.94995373 |
| S | 10.0934987 | -0.9496284 | 2.794858 |
| P | 7.3926002 | -1.8401921 | 4.94436823 |
| P | 8.44191492 | 1.99367145 | 2.60652519 |
| O | 9.98367169 | 1.17660664 | 5.98769749 |
| C | 9.29467223 | 0.70221052 | 5.1414714 |
| C | 9.50597863 | -1.4770965 | 1.21782976 |
| C | 8.17740096 | -1.4334593 | 0.87392796 |
| C | 10.6133398 | -1.9311692 | 0.30028047 |
| C | 7.63816685 | -2.017457 | -0.4132675 |
| F | 10.3216672 | -3.0862905 | -0.3391134 |
| F | 11.7591486 | -2.1463741 | 0.98569144 |
| F | 10.9040934 | -1.0053379 | -0.6521815 |
| F | 6.39461775 | -1.5712045 | -0.6834085 |
| F | 7.56526711 | -3.3696469 | -0.3553758 |
| F | 8.40374901 | -1.7065374 | -1.4863934 |
| C | 7.1624249 | 2.62683128 | 3.74348857 |
| C | 5.94136542 | 1.89134139 | 3.8039506 |
| C | 5.06806583 | 2.06846279 | 4.89223269 |
| C | 5.39250092 | 2.96908002 | 5.91767116 |
| C | 6.59183609 | 3.70688549 | 5.85511282 |
| C | 7.47844956 | 3.53282359 | 4.78362074 |
| C | 7.89521826 | 2.06052082 | 0.88225334 |
| C | 8.76636533 | 1.47982546 | -0.0640643 |
| C | 8.3784418 | 1.38855048 | -1.4072979 |
| C | 7.12517817 | 1.88253103 | -1.8115628 |
| C | 6.26910558 | 2.48729085 | -0.8739522 |
| C | 6.65216167 | 2.57884236 | 0.4748283 |
| C | 9.91909893 | 3.03911948 | 2.70416373 |
| C | 9.85498199 | 4.43004623 | 2.47103102 |
| C | 11.0222231 | 5.20485347 | 2.54831776 |
| C | 12.2558019 | 4.59067505 | 2.83975098 |
| C | 12.3227078 | 3.20213907 | 3.0485058 |
| C | 11.1560623 | 2.4228082 | 2.98525399 |
| C | 7.28625578 | -3.4110327 | 4.01274103 |

| | | | |
|---|---|---|---|
| C | 6.15234862 | -4.2468357 | 4.05973332 |
| C | 6.11319962 | -5.4210516 | 3.28906819 |
| C | 7.20105321 | -5.7647282 | 2.46612695 |
| C | 8.34162245 | -4.942803 | 2.43555593 |
| C | 8.3887693 | -3.7786798 | 3.2141211 |
| C | 5.64853113 | -1.4519628 | 5.38015071 |
| C | 5.22612805 | -1.1890433 | 6.69754054 |
| C | 3.88815136 | -0.8436144 | 6.95664109 |
| C | 2.95710033 | -0.7750083 | 5.9066229 |
| C | 3.37291609 | -1.0428643 | 4.58818476 |
| C | 4.70985173 | -1.3711063 | 4.32447068 |
| C | 8.20076657 | -2.2859646 | 6.52140201 |
| C | 8.46131434 | -1.2727831 | 7.47121642 |
| C | 9.09681018 | -1.5811264 | 8.68360122 |
| C | 9.49621 | -2.9028167 | 8.95426432 |
| C | 9.24784373 | -3.9139527 | 8.01012302 |
| C | 8.59763294 | -3.6092392 | 6.80197405 |
| H | 5.68622965 | 1.19587724 | 2.99423227 |
| H | 4.14082131 | 1.48743479 | 4.93511162 |
| H | 4.71434549 | 3.09669162 | 6.77003016 |
| H | 6.84449424 | 4.41192571 | 6.65667485 |
| H | 8.43057786 | 4.07534289 | 4.76510976 |
| H | 9.72934202 | 1.06905172 | 0.25750282 |
| H | 9.04597217 | 0.90578242 | -2.1284853 |
| H | 6.81566164 | 1.79801893 | -2.8606425 |
| H | 5.29569325 | 2.881374 | -1.1899593 |
| H | 5.97630346 | 3.03536206 | 1.20734016 |
| H | 8.89453297 | 4.90262528 | 2.22846449 |
| H | 10.9713821 | 6.2867498 | 2.37508194 |
| H | 13.167974 | 5.19742631 | 2.89680065 |
| H | 13.2853786 | 2.7214785 | 3.2610813 |
| H | 11.1901628 | 1.33256996 | 3.1080881 |
| H | 5.29457098 | -3.9795197 | 4.6871339 |
| H | 5.22439774 | -6.063699 | 3.32527834 |
| H | 7.15770276 | -6.6710271 | 1.84943092 |
| H | 9.18883579 | -5.18872 | 1.7843869 |
| H | 9.26389324 | -3.1187443 | 3.18177618 |
| H | 5.93570338 | -1.2576264 | 7.52982547 |
| H | 3.57318465 | -0.6363976 | 7.98678474 |

| | | | |
|---|---|---|---|
| H | 1.91231401 | -0.5120729 | 6.11298274 |
| H | 2.65598082 | -0.9913332 | 3.75975743 |
| H | 5.04736225 | -1.559956 | 3.29736287 |
| H | 8.16579783 | -0.2384962 | 7.26454342 |
| H | 9.28855401 | -0.785113 | 9.41328371 |
| H | 10.0025088 | -3.1422105 | 9.8972707 |
| H | 9.55964374 | -4.9459848 | 8.21217262 |
| H | 8.40177981 | -4.4041088 | 6.07266763 |

**Movie S1.** Video of low frequency vibrational modes for **1** in which nuclear displacements align with an isomerization pathway to **0**.

**Movie S2.** Video of low frequency vibrational modes for **0** in which nuclear displacements align with an isomerization pathway to **1**.

**Movie S3.** Video of low frequency vibrational modes for **0** in which nuclear displacements align with an isomerization pathway to **2**.

**Movie S4.** Video of low frequency vibrational modes for **2** in which nuclear displacements align with an isomerization pathway to **0**.

**REFERENCES**


(1) Balch, A. L.; Miller, J., *Inorg. Chem.* **1971,** *10*, 1410-1415.
(2) Krespan, C. G., *J. Am. Chem. Soc.* **1961,** *83*, 3434-3437.
(3) Neese, F., *J. Comput. Chem.* **2003,** *24*, 1740–1747.
(4) Kossmann, S.; Neese, F., *Chem. Phys. Lett.* **2009,** *481*, 240–243.
(5) Neese, F.; Wennmohs, F.; Hansen, A.; Becker, U., *Chem. Phys.* **2009,** *356*, 98–109.
(6) Izsák, R.; Neese, F., *J. Chem. Phys.* **2011,** *135*, 144105.
(7) Neese, F., *Wiley Interdisciplinary Reviews: Computational Molecular Science* **2012,** *2*, 73–78.
(8) Huzinaga, S.; Andzelm, J.; Radzio-Andzelm, E.; Sakai, Y.; Tatewaki, H.; Klobukiwski, M., *Gaussian Basis Sets for Molecular Calculations*. Elsevier Science: 1983; Vol. 16, p 434.
(9) Andrae, D.; Häußermann, U.; Dolg, M.; Stoll, H.; Preuß, H., *Theor. Chem. Acc.* **1990,** *77*, 123–141.
(10) Schäfer, A.; Horn, H.; Ahlrichs, R., *J. Chem. Phys.* **1992,** *97*, 2571–2577.
(11) Schäfer, A.; Huber, C.; Ahlrichs, R., *J. Chem. Phys.* **1994,** *100*, 5829–5835.
(12) Weigend, F., *Phys. Chem. Chem. Phys.* **2006,** *8*, 1057–1065.
(13) Pantazis, D. A.; Neese, F., *Theor. Chem. Acc.* **2012,** *131*, 1292.
(14) Pantazis, D. A.; Neese, F., *J. Chem. Theory Comput.* **2011,** *7*, 677-684.
(15) Pantazis, D. A.; Neese, F., *J. Chem. Theory Comput.* **2009,** *5*, 2229-2238.
(16) Pantazis, D. A.; Chen, X.-Y.; Landis, C. R.; Neese, F., *J. Chem. Theory Comput.* **2008,** *4*, 908-919.
(17) Sinnecker, S.; Rajendran, A.; Klamt, A.; Diedenhofen, M.; Neese, F., *J. Phys. Chem. A* **2006,** *110*, 2235–2245.
(18) Grimme, S.; Ehrlich, S.; Goerigk, L., *J. Comput. Chem.* **2011,** *32*, 1456–1465.
(19) Grimme, S.; Antony, J.; Ehrlich, S.; Krieg, H., *J. Chem. Phys.* **2010,** *132*, 154104.
(20) Pettersen, E. F.; Goddard, T. D.; Huang, C. C.; Couch, G. S.; Greenblatt, D. M.; Meng, E. C.; Ferrin, T. E., *J. Comput. Chem.* **2004,** *25*, 1605–1612.
(21) Shim, S.-H.; Strasfeld, D. B.; Fulmer, E. C.; Zanni, M. T., *Opt. Lett.* **2006,** *31*, 838-840.
(22) Shim, S.-H.; Zanni, M. T., *Phys. Chem. Chem. Phys.* **2009,** *11*, 748-761.
(23) Nee, M. J.; McCanne, R.; Kubarych, K. J.; Joffre, M., *Opt. Lett.* **2007,** *32*, 713-715.
(24) Rock, W.; Li, Y.-L.; Pagano, P.; Cheatum, C. M., *J. Phys. Chem. A* **2013,** *117*, 6073-6083.
(25) Hommel, E. L.; Allen, H. C., *Anal. Sci.* **2001,** *17*, 137-139.
(26) Laaser, J. E.; Xiong, W.; Zanni, M. T., *J. Phys. Chem. B* **2011,** *115*, 2536-2546.
(27) Zheng, J.; Kwak, K.; Asbury, J.; Chen, X.; Piletic, I. R.; Fayer, M. D., *Science* **2005,** *309*, 1338.
(28) Kwak, K.; Zheng, J.; Cang, H.; Fayer, M. D., *J. Phys. Chem. B* **2006,** *110*, 19998-20013.
(29) Hamm, P.; Zanni, M. T., *Concepts and methods of 2D Infrared Spectroscopy*. Cambridge University Press: New York, 2011.